

# Effect of alkyl chain length on chemical sensing of polydiacetylene and polydiacetylene/ZnO nanocomposites

Aide Wu · Yuan Gu · Huiquan Tian · John F. Federici ·  
Zafar Iqbal

Received: 13 May 2014 / Revised: 14 July 2014 / Accepted: 31 July 2014 / Published online: 12 August 2014  
© Springer-Verlag Berlin Heidelberg 2014

**Abstract** Polydiacetylenes (PDAs) and PDA/ZnO nanocomposites based on the monomers 10,12-pentacosadiynoic acid (PCDA), 10,12-tricosadiynoic acid (TCDA), and 10,12-docosadiynedioic acid (DCDA) monomers have been investigated for chromatic chemical sensing of a number of organic liquids. Chromatic sensitivity is associated with the interaction of the organic liquid with the PDA side chain to give rise to the strain-induced blue to red colorimetric transition. Attenuated total reflection (ATR) Fourier transform infrared (FTIR) spectroscopy demonstrated that in the PDA/ZnO nanocomposites, the PDA side chains form chelates with ZnO. The chromatic properties of PDAs and PDA/ZnO composites in organic liquids, to certain extent, depend on the side-chain length and the number of carboxylic head groups. Pure PDAs and PDA/ZnO nanocomposites in different organic liquids studied by Raman spectroscopy show that the chromatic selectivity of PDAs for certain organic liquids with respect to the blue to red phase transition is closely related to the

side-chain structure of the PDAs. Moreover, the interactions are stronger with those PDAs where the blue to red transition is irreversible. Density functional theory (DFT) simulations show that the chromatic sensitivity of the PDAs toward a particular organic correlates with the C–C bond torsion angle of the PDA backbone.

**Keywords** Conjugated polymer · Nanocomposite · Chemosensor · DFT simulation

## Introduction

As chromatic sensor materials, polydiacetylenes (PDAs) have drawn tremendous attention due to their unique blue to red colorimetric transition, which can be triggered by mechanical, temperature, and chemical stimuli [1–8]. The featured chromic transition of PDAs could be either irreversible or reversible depending on the chemical structure and interaction of pendant side chain. The strain on the backbone induced by external stimuli leads to the red phase formation from blue phase via side-chain head group interactions. When strong head group interactions are present in PDA molecule, the red phase could rapidly reverse back to blue phase on removing the stimuli [9–14]. The irreversible red phase is due to the side chain failed to release the induced strain. The solid-state topotactic photo-polymerization of diacetylene monomers by exposure to UV or  $\gamma$ -radiation makes the synthesis of the PDAs more convenient and widespread for use in applications [15, 16]. Thermochromism in closely packed and uniformly ordered thin films of various PDAs are well known [17] and have been widely studied for temperature-sensing

**Electronic supplementary material** The online version of this article (doi:10.1007/s00396-014-3365-y) contains supplementary material, which is available to authorized users.

A. Wu (✉) · Y. Gu · J. F. Federici  
Department of Physics, New Jersey Institute of Technology, Newark,  
NJ 07102, USA  
e-mail: aw49@njit.edu

Z. Iqbal  
Department of Chemistry and Environmental Science, New Jersey  
Institute of Technology, Newark, NJ 07102, USA

H. Tian  
Key Laboratory of Computational Geodynamics, University of  
Chinese Academy of Science, Beijing 100049, China

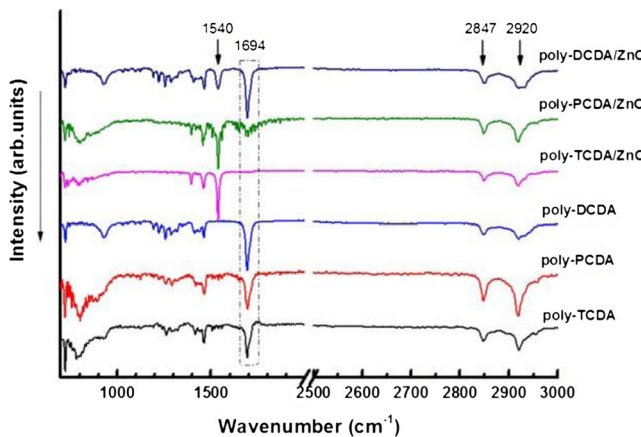


**Fig. 1** ATR-FTIR spectra at room temperature in the blue phase of poly-DCDA, poly-PCDA, and poly-TCDA and their corresponding ZnO composites

applications [18–22]. Recent studies on enhancing the electrical conductivity of PDAs have broadened electrochromic applications of PDAs [23–25]. However, little attention has been paid to a systematic study of the use of PDAs in chemical sensing. Most studies have been conducted on polymers obtained from PDA monomers with one carboxylic group on the side chain, such as in 10,12-pentacosadiynoic acid (PCDA) and 10,12-tricosadiynoic acid (TCDA) [7, 18–20, 22]; however, PDA monomers with two carboxylic groups, such as 10,12-docosadiynedioic acid (DCDA), have not been investigated for chemical sensing.

Previous research on poly-PCDA/ZnO and poly-TCDA/ZnO nanocomposites provided a broad understanding of the changes in chromatic properties of the

nanocomposites relative to those of the pure polymer [26, 27]. In this paper, further investigations have been carried out to study the phase transition of PDAs and PDA/ZnO nanocomposites when exposed to different organic liquids. Raman spectroscopy was used to characterize the PDAs and PDA/ZnO nanocomposites, together with attenuated total reflection Fourier transform infrared (ATR-FTIR) studies at ambient temperature and density functional theory simulations to obtain a molecular-level understanding of the colorimetric changes. In addition, colorimetric measurements were performed using photographic processing software to quantify the chromatic changes.

## Experimental section

### Materials

TCDA, PCDA, and DCDA were purchased from GFS Chemicals, and nanocrystalline ZnO (<100-nm diameter) was purchased from Sigma-Aldrich. Analytical-grade chloroform was purchased from Sigma-Aldrich and used without further purification.

### Synthesis of PDA/ZnO nanocomposites

PDA/ZnO suspensions were prepared by suspending 0.045-mMol equivalent of ZnO in 10-mM solution of the PDA monomer in chloroform. The suspension contained in a beaker was sonicated in a water bath at room temperature for 30 min and dried at 40 °C with magnetic stirring for 8 h. The magnetic stirring was stopped after the solid state was achieved. The pure PDA monomer and PDA monomer/ZnO composites were polymerized to the blue phase of PDA and PDA/ZnO composite by irradiating with a 254-nm wavelength UV source. Powders of the blue phase composite were obtained by scraping from the beaker and grinding into a fine powder. Red phase composite powders were similarly produced and suspended in different organic liquids.

### Raman spectroscopy

Raman spectra were obtained using a Mesophotonics Raman spectrometer with 785-nm laser excitation. The spectrometer was calibrated using a silicon wafer and diamond powder standards to a frequency accuracy of 1 cm<sup>-1</sup>. Thick films for the Raman measurements were prepared by mixing suspensions of PDA monomer with ZnO, using chloroform as the suspension medium. After drying and 254-nm UV irradiation, Raman spectra from the dry powders of PDA and PDA/ZnO

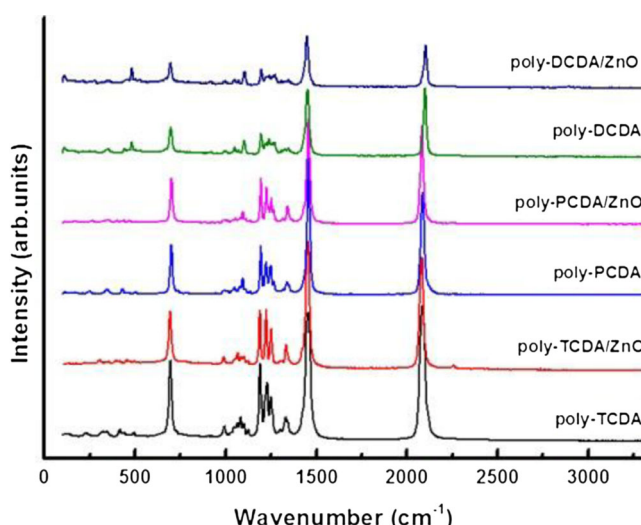


**Fig. 2** Raman spectra of poly-DCDA, poly-PCDA, and poly-TCDA and their corresponding ZnO nanocomposites in the blue phase at room temperature

**Table 1** Polymer backbone Raman frequencies for different PDAs and corresponding PDA/ZnO nanocomposites in the blue phase in the presence of organic liquids

Organic liquid	Frequencies ( $\text{cm}^{-1}$ )					
	C=C	C≡C	C=C	C≡C	C=C	C≡C
	Poly-TCDA					
None	1,456	2,084	1,457	2,086/2,124*	1,452	2,102
Methanol	1,458/1,524	2,084/2,124	1,457	2,096/2,124*	1,446	2,102
Ethanol	1,456/1,524	2,084/2,124	1,457/1,522*	2,090/2,124*	1,446	2,102
Benzyl alcohol	1,456/1,522	2,082/2,124	1,457/1,522	2,086/2,124*	1,442	2,098
Octanol	1,454/1,518	2,080/2,120	1,457/1,522	2,086/2,122*	1,444	2,100
Diethyl ether	1,522/1,456*	2,126/2,084*	1,457/1,522	2,086/2,124	1,444	2,100
DMF	1,524	2,124	1,457*/1,522	2,086*/2,126	1,522/1,444*	2,120
DCM	1,522	2,126	1,457/1,520	2,086/2,126	1,444	2,100
THF	1,522	2,124	1,524	2,124	1,520*/1,446	2,120*/2,102
Acetone	1,524/1,458	2,126/2,082	1,457/1,522	2,090/2,122*	1,444	2,102
	Poly-TCDA/ZnO					
None	1,454	2,082	1,456	2,084	1,448	2,104
Methanol	1,458/1,524*	2,084/2,118*	1,456	2,084	1,446	2,084/2,104*
Ethanol	1,458/1,524*	2,086/2,122*	1,456/1,522*	2,084/2,124*	1,446	2,080/2,104*
Benzyl alcohol	1,458/1,522*	2,086/2,124*	1,456/1,522*	2,084	1,444	2,078
Octanol	1,454/1,518*	2,082/2,118*	1,456	2,084	1,446	2,078
Diethyl ether	1,458/1,522*	2,086/2,124*	1,456/1,522*	2,084/2,124*	1,444	2,100
DMF	1,456/1,520*	2,082/2,124*	1,456/1,522*	2,084/2,126*	1,444	2,076
DCM	1,458/1,522*	2,086/2,126*	1,456/1,520*	2,086/2,126*	1,446	2,080/2,104*
THF	1,456/1,522*	2,084/2,118*	1,456/1,524*	2,084/2,124*	1,446	2,080
Acetone	1,456/1,524*	2,084/2,124*	1,456/1,522*	2,084/2,122*	1,444	2,080/2,104*

“\*” represents a shoulder

DMF dimethylformamide, DCM dichloromethane, THF tetrahydrofuran

were measured on a silicon wafer. The effect of organic liquids on the PDAs were carried out by suspending the same molar amounts of PDA or PDA/ZnO in 4 ml of the organic liquid and measuring the Raman spectra after 5 min of bath sonication of the suspension.

#### ATR-FTIR spectroscopy

ATR-FTIR was carried out using a Nicolet ThermoElectron FTIR 560 spectrometer with a MIRacle ATR platform assembly and a Ge plate.

RGB measurements of poly-PCDA and poly-PCDA/ZnO at different temperatures

The “red phase” and “blue phase” defined by Raman spectroscopy are based on the vibration modes of molecular structures of PDAs, which means, especially in the blue phase and red phase coexisting system, Raman spectra could not tell the exact overall color as the one

detected by human eye. Thus, for precise colorimetric information, the photographic images of PDAs or PDA/ZnO composites in an organic liquid were quantitatively analyzed by photographic processing software to obtain the RGB values obtained from the combination of red, green, and blue colors.

#### Results and discussion

##### ATR-FTIR spectroscopy

Based on our previous studies [26, 27], ATR-FTIR can provide information on chemical interactions between the PDA side chain in poly-PCDA/ZnO and poly-TCDA/ZnO. To confirm if poly-DCDA/ZnO shows similar behavior, FTIR spectroscopy was carried out on this nanocomposite and also, for comparison, on poly-PCDA/ZnO and poly-TCDA/ZnO. The effect of the side-chain head group and ZnO interaction is reflected

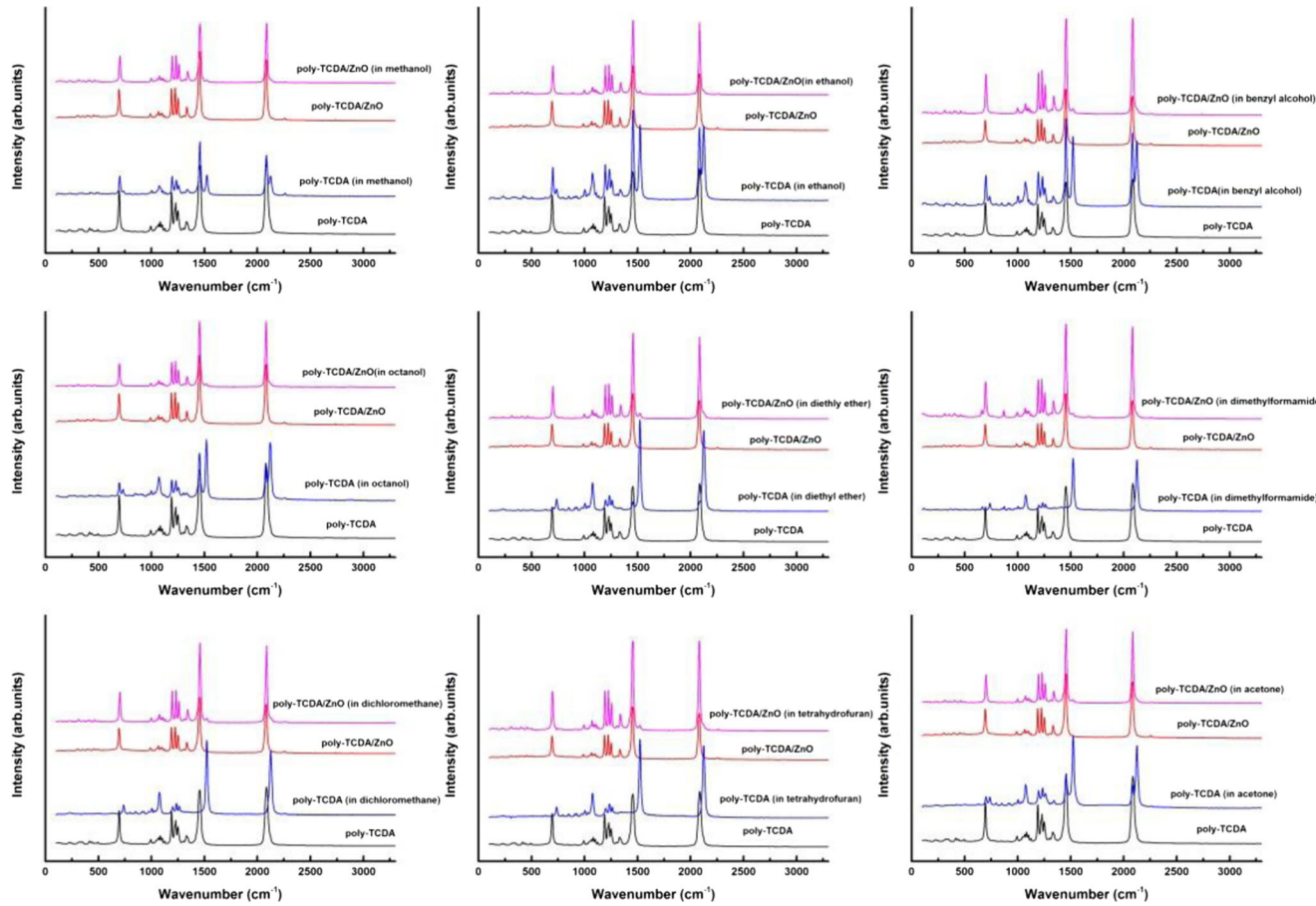


**Fig. 3** Raman spectra of poly-TCDA and poly TCDA/ZnO in the blue phase and in different organic liquids

in the FTIR spectra shown in Fig. 1. In the  $700\text{--}3,000\text{ cm}^{-1}$  spectral region, lines at  $2,920$  and  $2,847\text{ cm}^{-1}$  can be assigned to the asymmetric and symmetric stretching vibrations, respectively, of the  $\text{CH}_2$  groups on the side chains; the lines at  $1,463$  and  $1,417\text{ cm}^{-1}$  can be assigned to  $\text{CH}_2$  scissoring modes; and the line at  $1,694\text{ cm}^{-1}$  can be attributed to the hydrogen-bonded carbonyl  $\text{C=O}$  stretching vibration. A relatively strong line appears at  $1,540\text{ cm}^{-1}$  in the spectra of PDA/ZnO composites together with a concomitant decrease in intensity of the  $\text{C=O}$  stretching line at  $1,694\text{ cm}^{-1}$ . This  $1,540\text{ cm}^{-1}$  line can be assigned to an asymmetric  $\text{COO}^-$  stretching vibration and its presence in the spectra together with the corresponding decrease in the intensity of the  $\text{C=O}$  stretching line can be attributed to the formation of a chelate between neighboring side-chain  $-\text{COOH}$  head groups of the PDAs and  $\text{Zn}^{2+}$  ions from ZnO, in agreement with previous work [26, 27]. However, comparing different PDA/ZnO composites under the same stoichiometric ratio of PDA to ZnO, even though chelate formation between PDA and ZnO are indicated in the ATR-FTIR spectra, the  $\text{C=O}$  line at  $1,694\text{ cm}^{-1}$  decreases in

intensity to different degrees. For example, there is no evidence of the  $\text{C=O}$  line in the FTIR spectrum of poly-TCDA/ZnO. Also, the  $\text{C=O}$  line is very weak in poly-PCDA/ZnO but remains relatively strong in poly-DCDA/ZnO (Fig. 1). This suggests that chelation occurs only at one  $-\text{COOH}$  head group in poly-DCDA/ZnO and at the one available  $-\text{COOH}$  head group present in both poly-TCDA and poly-PCDA.

#### Raman spectroscopy

Raman scattering due to the molecular vibrational modes of the conjugated polymer backbone are expected to be primarily resonance-enhanced for excitation using 780-nm laser radiation. From the Raman spectra in Fig. 2 for the pure PDAs in the blue phase, two intense lines near  $2,100$  and  $1,450\text{ cm}^{-1}$  are observed at room temperature in the blue phase, which can be definitively assigned to the  $\text{C}\equiv\text{C}$  and  $\text{C=C}$  stretching modes of the polymer backbone, respectively. However, there are small but measureable differences in the  $\text{C}\equiv\text{C}$  and  $\text{C=C}$  stretching mode frequencies for the different PDAs as summarized in Table 1. The  $\text{C=C}$  stretching

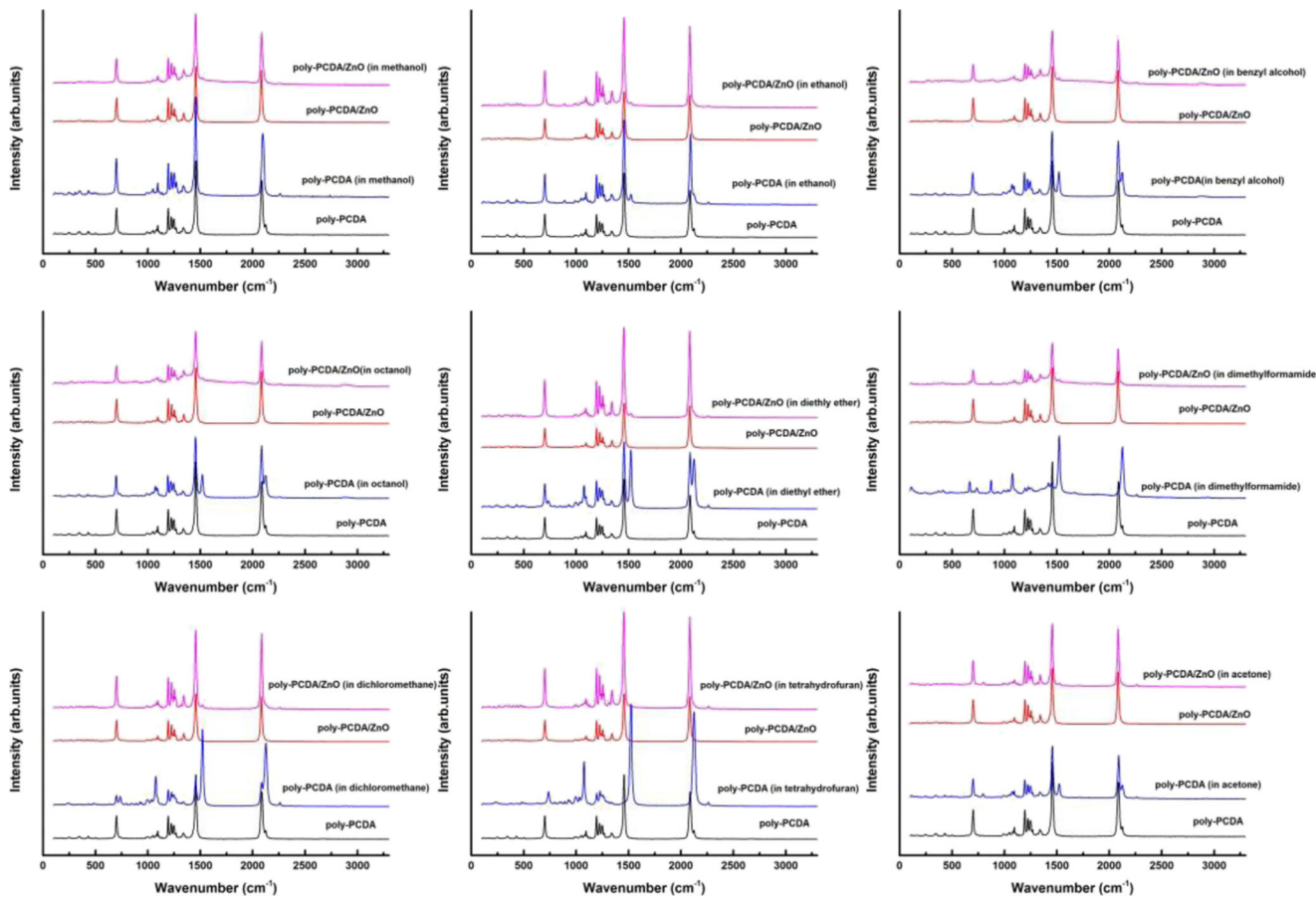


**Fig. 4** Raman spectra of poly-PCDA and poly PCDA/ZnO in the blue phase and in different organic liquids

mode frequencies for poly-TCDA and poly-PCDA are essentially the same within  $\pm 1 \text{ cm}^{-1}$ , whereas the C≡C stretching mode frequencies shows a small  $2 \text{ cm}^{-1}$  upshift and the appearance of a shoulder at  $2,124 \text{ cm}^{-1}$  in poly-PCDA that is most likely due to the presence of a red phase impurity in the sample [26]. The C≡C stretching mode frequency in poly-DCDA is, however, 16 and  $18 \text{ cm}^{-1}$  higher than that for poly-PCDA and poly-TCDA, respectively, indicating a higher strain on the polymer backbone in poly-DCDA associated with the presence of two –COOH head groups on its side chains. Chelate formation between PDA and ZnO in poly-TCDA/ZnO and poly-PCDA/ZnO results in a small frequency downshift for both the C≡C and C=C stretching modes relative to that of the pure polymer due to a small decrease in strain on the polymer backbone. By contrast, in poly-DCDA/ZnO, there is a  $4 \text{ cm}^{-1}$  downshift in the C=C stretching mode frequency but a  $2 \text{ cm}^{-1}$  upshift in the C≡C stretching mode frequency, probably linked to the presence of two –COOH head groups in poly-DCDA (also, see further discussion in the section “Density functional theory simulations”).

In order to evaluate the use of the PDAs and PDA/ZnO nanocomposites as chromatic chemical sensors, Raman spectroscopy was carried out to study the effect of organic liquids on the Raman spectra of the PDAs and PDA/ZnO nanocomposites. Methanol, ethanol, benzyl alcohol, octanol, diethyl ether, dimethylformamide (DMF), dichloromethane (DCM), tetrahydrofuran (THF), and acetone (analytical grade from Sigma-Aldrich) were selected as organic liquids to trigger a color change. The results are shown in Figs. 3, 4, and 5 and the observed C≡C and C=C stretching mode frequencies of the PDAs in the organic liquids are listed in Table 1.

From Fig. 3, it is evident that the C≡C and C=C stretching mode lines of poly-TCDA and poly-TCDA-ZnO are either split by the appearance of a line at higher frequency due to the partial conversion to the red phase or shift to higher frequencies due to complete conversion to the red phase, depending on the organic liquid added. Poly-TCDA showed a peak splitting in the C≡C and C=C stretching mode regions of the Raman spectrum due to partial formation of the red phase when

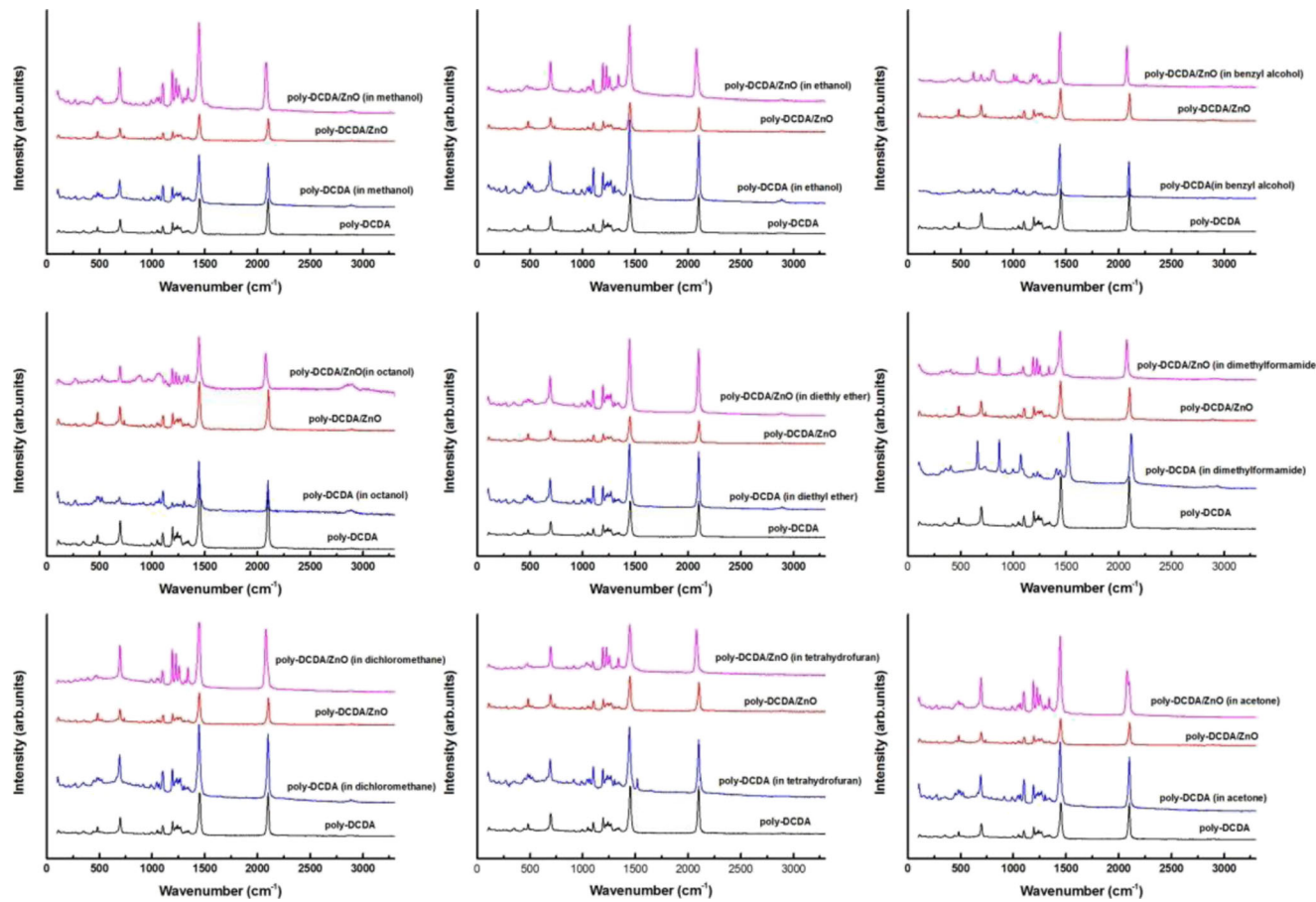


**Fig. 5** Raman spectra of poly-DCDA and poly DCDA/ZnO in the blue phase and in different organic liquids

alcohols and acetone are present, while in DMF, DCM, and THF, the C≡C and C=C Raman peaks increase in frequency to new values due to complete conversion of the blue to the red phase. In the presence of diethyl ether, a small shoulder due to the blue phase remains at a lower frequency although conversion to the red phase is complete. For poly-TCDA/ZnO, only a high-frequency shoulder is formed in the presence of all the selected organic liquids, indicating that conversion to the red phase is not complete. The unchanged blue phase is likely to be due to chelate formation between neighboring side chains in the nanocomposites which could stand up with the chemical stimuli.

The behavior of the Raman spectra of blue poly-PCDA and poly-PCDA/ZnO nanocomposite in different organic liquids is similar to that of poly-TCDA and its corresponding ZnO nanocomposite, except for the absence of red phase formation in methanol. For the other three alcohols, only weak red phase lines are observed.

The Raman spectra of poly-DCDA and poly-DCDA/ZnO in different organic liquids are shown in Fig. 5. By contrast to the results of poly-TCDA and poly-PCDA, poly-DCDA shows a small downshift in the C=C

stretching mode frequency in the presence of organic liquids possibly due to chemical interaction with the organic liquids (except in DMF and THF). For the C≡C stretching mode, the upshift due to red phase formation is only observed in DMF and THF, while in most other liquids, the C≡C stretching mode frequency either remains the same (as in methanol, ethanol, and acetone) or downshifts slightly (as in benzyl alcohol, octanol, diethyl ether, and DCM). Compared with poly-DCDA, the downshift of the C≡C peak frequencies for poly-DCDA/ZnO is much larger in the presence of the organic liquids (for example, from 2,104 to about 2,080 cm<sup>-1</sup>), whereas the C=C peak frequency downshift is small (from 1,448 to about 1,445 cm<sup>-1</sup>).

An important feature worth noting is that the blue to red transition of PDAs induced by the organic liquids are all irreversible, but the organic liquid-induced red phase for all three PDA/ZnO nanocomposites are reversible; the red phase peaks appear in organic liquid environment, and once the PCDA/ZnO composites are taken out from the organic liquid, only characteristic peaks of blue phase could be found in the spectra (please see supplementary materials). This can be attributed to

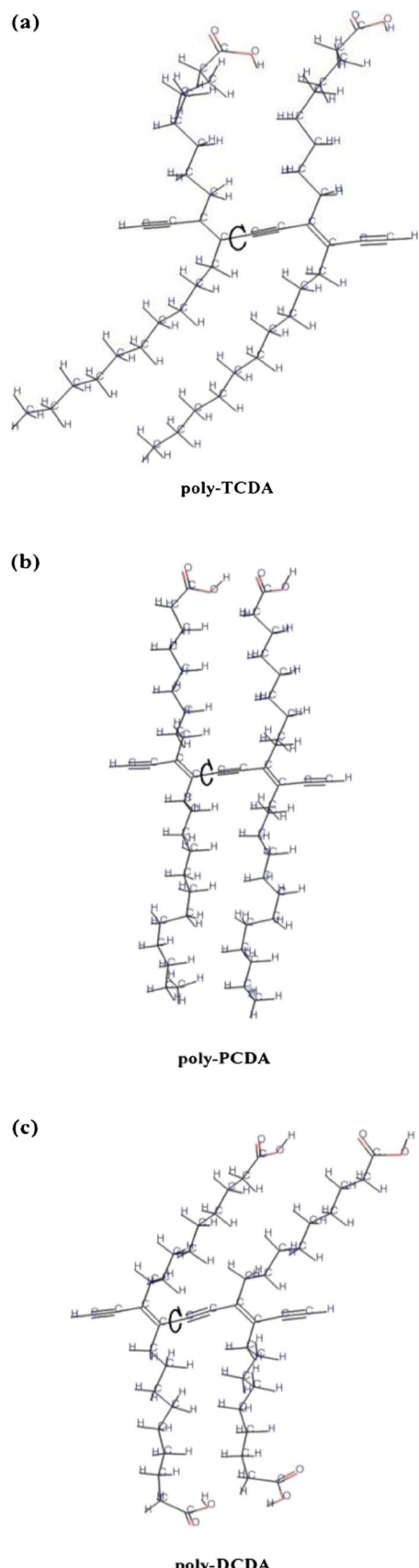


**Fig. 6** Structures of simulated PDA segments: **a** poly-TCDA, **b** poly-PCDA, and **c** poly-DCDA

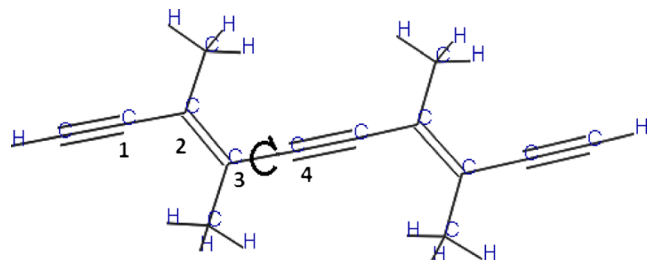


**Fig. 7** Structure of the PDA segment used for the C–C torsion angle study

strong chelation interactions comparable to chemical bonding in the PDA/ZnO nanocomposites that provides greater stability to the blue relative to the red phase.

#### Density functional theory simulations

Density functional theory (DFT) simulations were carried out to understand the interesting chemical sensing behaviors of the PDAs and PDA/ZnO composites in terms of their molecular structure properties. The simulations were carried out using Material Studio 4.3 (Accelrys Software Inc.) with B3LYP (DND basis set) function in DMol3 modules which is a counterpart of the 6-31G\* basis set of Gaussian 3.0. On balancing between the accuracy and number of computations needed, a medium-accuracy-level calculation was selected for the simulations.

For construction of the molecular structure, consideration was given to the amount of computation needed and limitation of the Linux cluster available to carry out the simulations. Segments of the polymers shown in Fig. 6, which are equivalent to molecules with a polymerization degree of 2, were used for this simulation. The main difference between the PDAs is the torsion angle of the single bond on the polymer backbone as indicated in Fig. 7. This is probably due to the fact that the backbone carbon chain of the PDAs is in the zigzag conformation with the possibility that torsion occurs on the carbon-carbon single bond. In order to clearly show the torsion angle of the carbon single bond for different

**Table 2** C–C torsion angle on the PDA backbones

Trial number	C–C torsion angle (°)		
	Poly-TCDA	Poly-PCDA	Poly-DCDA
1	49.018	39.746	7.561
2	48.176	39.862	8.012
3	49.694	40.354	7.402
4	50.402	38.708	6.986
5	48.464	39.454	7.124

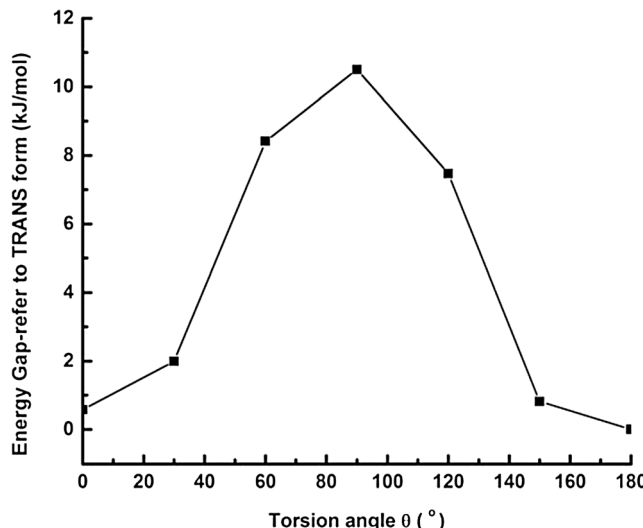


**Fig. 8** Potential energy curve as a function of torsion angle around the central C–C bond in *cis*-carbon with reoptimization of other geometrical parameters as discussed in the text

PDAs, a *cis*-structured backbone is set as the 0° reference point. Also, each PDA was constructed and simulated five times to make sure that the conformation of the side chains is in a random state. The results showed that the C–C bond torsion angles surprisingly fall within a certain small range from about 48° to 50° for TCDA, about 38° to 40° for PCDA, and about 7° to 8° for DCDA as shown in Table 2.

Due to the coincidence of C–C torsion angles in the simulations, it is obvious that the backbone structure of the PDAs is closely related to that of the side chain. In order to investigate the torsion on the backbone, the structure as shown in Fig. 7 was adopted using a methyl group instead of the side chain. The basic idea was to determine how the torsion of the C–C bond affects the backbone structure; therefore, in this simulation, the potential energy of this structure was considered as the criterion to evaluate the C–C bond torsion. The *trans*-structure was set as a reference potential energy point, and the potential energy was calculated with the B3LYP/6-31G\* function using C3-C4 torsions angles of 30°, 60°, 90°, 120°, 150°, and 180° while other C–C torsion angles were restricted.

The results of the potential energy calculation are plotted in Fig. 8, which shows that the maximum energy refers to a *cis*-structure which appears when  $\theta=90^\circ$ . This plot generally demonstrates how the C–C bond torsion angle affects the backbone system. It can also explain how PDAs with different side chains would exhibit different chromatic and spectroscopic changes discussed above (also, see the “RGB measurements” section). For example, the longer the C–C bond, the

**Fig. 9** Array of cropped photographic images of PDAs and PDA/ZnO nanocomposites in selected organic liquids (*top panel*) and histogram of RGB values of the photographic images analyzed by software (*bottom panel*) ▶

less stress is needed to induce a chromatic transition in the PDA, which is consistent with the fact that poly-TCDA is the most chromatically sensitive to the organic liquids evaluated.

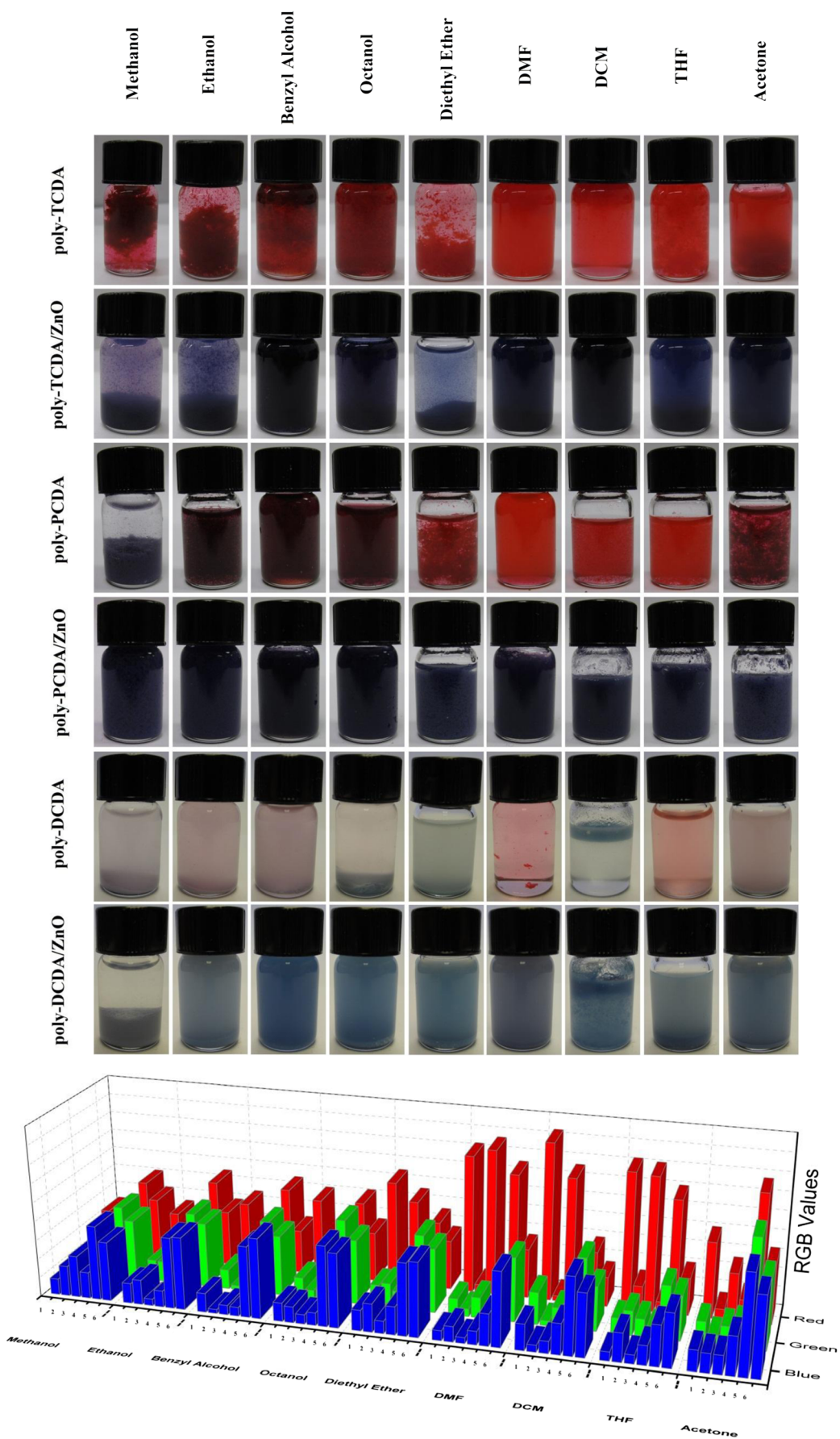
#### RGB measurements

To demonstrate the selective sensing capabilities of the PDAs which could be detected by human eye, RGB measurements were conducted to quantitatively evaluate the color of the PDAs and PDA/ZnO composites in the presence of selected organic liquids. From Fig. 9, it can be seen that poly-TCDA turned red on contacting an organic liquid corresponding to a higher red value than green and blue values. Similar phenomena were observed for poly-PCDA samples (except in methanol). However, poly-DCDA only shows a distinguishable red value when DMF and THF are present, indicating that the chemical recognition ability of PDAs is closely related to the chemical structure of the side chains on the PDA backbone.

It was also observed that all the PDA/ZnO nanocomposites show similar RGB values with different degrees of blue color in the presence of different organic liquids. This indicates that the chelates formed in PDA/ZnO nanocomposites involve a strong chemical bond and can therefore withstand chemical stress to maintain the blue phase (as shown by the Raman data) in the presence of the selected organic liquids.

#### Conclusions

PDAs based on the monomers PCDA, TCDA, and DCDA and their nanocomposites with ZnO were evaluated for potential use as chemical sensors for selected organic liquids. Chromatic sensitivity evaluated by Raman spectral data and quantitatively RGB analyses were found to be associated with the interaction of the organic liquids with the PDA side chain to give rise to the blue to red colorimetric transition. ATR-FTIR spectral data show that chelate formation occurs only on one of the two carboxylic head groups in poly-DCDA/ZnO. Due to strong chemical interactions between zinc and carboxylic ions during chelate formation that stabilize the blue phase, chromatic



sensitivity to organic liquids is low for PDA/ZnO nanocomposites. DFT simulations indicate that the chromatic sensitivity of the PDAs to a particular organic depends on the C–C bond torsion angle of the PDA backbone. Future studies will focus on the limit of chromatic detection of organic species by the PDAs and their nanocomposites investigated here.

**Acknowledgments** The authors acknowledge support by ARDEC, Picatinny Arsenal, and CarboMet LLC.

## References

1. Descalzo AB, Dolores Marcos M, Monte C, Martinez-Manez R, Rurack K (2007) Mesoporous silica materials with covalently anchored phenoxazinone dyes as fluorescent hybrid materials for vapour sensing. *J Mater Chem* 17:4716–4723
2. Janzen MC, Ponder JB, Bailey DP, Ingison CK, Suslick KS (2006) Colorimetric sensor arrays for volatile organic compounds. *Anal Chem* 78:3591–3600
3. Lu Y, Yang Y, Sellinger A, Lu M, Huang J, Fan H et al (2001) Self-assembly of mesoscopically ordered chromatic polydiacetylene/silica nanocomposites. *Nature* 410:913–917
4. Muro ML, Daws CA, Castellano FN (2008) Microarray pattern recognition based on PtII terpyridyl chloride complexes: vapochromic and vapoluminescent response. *Chem Commun* (46): 6134–6. doi: 10.1039/b812634h
5. Rakow NA, Suslick KS (2000) A colorimetric sensor array for odour visualization. *Nature* 406:710–713
6. Champaiboon T, Tumcharern G, Potisatityuenyong A, Wacharasindhu S, Sukwattanasinitt M (2009) A polydiacetylene multilayer film for naked eye detection of aromatic compounds. *Sensors Actuators B Chem* 139:532–537
7. Jiang H, Wang Y, Ye Q, Zou G, Su W, Zhang Q (2010) Polydiacetylene-based colorimetric sensor microarray for volatile organic compounds. *Sensors Actuators B Chem* 143:789–794
8. Pumtang S, Siripornnoppakhun W, Sukwattanasinitt M, Ajavakom A (2011) Solvent colorimetric paper-based polydiacetylene sensors from diacetylene lipids. *J Colloid Interface Sci* 364:366–372
9. Hammond PT, Rubner MF (1997) Thermochromism in liquid crystalline polydiacetylenes. *Macromolecules* 30:5773–5782
10. Huang X, Jiang S, Liu M (2004) Metal ion modulated organization and function of the Langmuir–Blodgett films of amphiphilic diacetylene: photopolymerization, thermochromism, and supramolecular chirality. *J Phys Chem B* 109:114–119
11. Peng H, Tang J, Pang J, Chen D, Yang L, Ashbaugh HS et al (2005) Polydiacetylene/silica nanocomposites with tunable mesostructure and thermochromatism from diacetylenic assembling molecules. *J Am Chem Soc* 127:12782–12783
12. Kim JM, Lee YB, Chae SK, Ahn DJ (2006) Patterned color and fluorescent images with polydiacetylene supramolecules embedded in poly(vinyl alcohol) films. *Adv Funct Mater* 16:2103–2109
13. Lee S, Kim JM (2007) Alpha-cyclodextrin: a molecule for testing colorimetric reversibility of polydiacetylene supramolecules. *Macromolecules* 40:9201–9204
14. Park H, Lee JS, Choi H, Ahn DJ, Kim JM (2007) Rational design of supramolecular conjugated polymers displaying unusual colorimetric stability upon thermal stress. *Adv Funct Mater* 17:3447–3455
15. Batchelder DN, Evans SD, Freeman TL, Haeussling L, Ringsdorf H, Wolf H (1994) Self-assembled monolayers containing polydiacetylenes. *J Am Chem Soc* 116:1050–1053
16. Baughman RH (1972) Solid-state polymerization of diacetylenes. *J Appl Phys* 43:4362–4370
17. Robert WC, Darryl YS, Matthew SM, Eriksson MA, Alan RB (2004) Polydiacetylene films: a review of recent investigations into chromogenic transitions and nanomechanical properties. *J Phys Condens Matter* 16:R679–R697
18. Chanakul A, Traiphol N, Traiphol R (2013) Controlling the reversible thermochromism of polydiacetylene/zinc oxide nanocomposites by varying alkyl chain length. *J Colloid Interface Sci* 389:106–114
19. Charoenthai N, Pattanatornchai T, Wacharasindhu S, Sukwattanasinitt M, Traiphol R (2011) Roles of head group architecture and side chain length on colorimetric response of polydiacetylene vesicles to temperature, ethanol and pH. *J Colloid Interface Sci* 360:565–573
20. Gou M, Guo G, Zhang J, Men K, Song J, Luo F et al (2010) Time-temperature chromatic sensor based on polydiacetylene (PDA) vesicle and amphiphilic copolymer. *Sensors Actuators B Chem* 150: 406–411
21. Ryu S, Yoo I, Song S, Yoon B, Kim J-M (2009) A thermoresponsive fluorogenic conjugated polymer for a temperature sensor in microfluidic devices. *J Am Chem Soc* 131:3800–3801
22. Traiphol N, Runguangviriya N, Potai R, Traiphol R (2011) Stable polydiacetylene/ZnO nanocomposites with two-steps reversible and irreversible thermochromism: the influence of strong surface anchoring. *J Colloid Interface Sci* 356:481–489
23. Peng H, Sun X, Cai F, Chen X, Zhu Y, Liao G et al (2009) Electrochromatic carbon nanotube/polydiacetylene nanocomposite fibres. *Nat Nanotechnol* 4:738–741
24. Yoon B, Ham D-Y, Yarimaga O, An H, Lee CW, Kim J-M (2011) Inkjet printing of conjugated polymer precursors on paper substrates for colorimetric sensing and flexible electrothermochromic display. *Adv Mater* 23:5492–5497
25. Gatebe E, Herron H, Zakeri R, Ramiah Rajasekaran P, Aouadi S, Kohli P (2008) Synthesis and characterization of polydiacetylene films and nanotubes. *Langmuir* 24:11947–11954
26. Patlolla A, Zunino J, Frenkel AI, Iqbal Z (2012) Thermochromism in polydiacetylene–metal oxide nanocomposites. *J Mater Chem* 22: 7028–7035
27. Wu A, Beck C, Ying Y, Federici J, Iqbal Z (2013) Thermochromism in polydiacetylene–ZnO nanocomposites. *J Phys Chem C* 117: 19593–19600